

Neuronal Excitability

# Subregional Differences in Medium Spiny Neuron Intrinsic Excitability Properties between Nucleus Accumbens Core and Shell in Male Rats

Cristina E. Maria-Rios,<sup>1</sup> Geoffrey G. Murphy,<sup>1,2,3</sup> and Jonathan D. Morrow<sup>1,2,4</sup><https://doi.org/10.1523/ENEURO.0432-22.2023>

<sup>1</sup>Neuroscience Graduate Program, University of Michigan, Ann Arbor, MI 48109, <sup>2</sup>Michigan Neuroscience Institute, University of Michigan, Ann Arbor, MI 48109, <sup>3</sup>Department of Molecular and Integrative Physiology, University of Michigan, Ann Arbor, MI 48109, and <sup>4</sup>Department of Psychiatry, University of Michigan, Ann Arbor, MI 48109

## Abstract

The nucleus accumbens (NAc) is known for its central role in reward and motivation (Day and Carelli, 2007; Floresco, 2015; Salgado and Kaplitt, 2015). Decades of research on the cellular arrangement, density, and connectivity of the NAc have identified two main subregions known as the core and shell (Záborszky et al., 1985; Berendse and Groenewegen, 1990; Zahm and Heimer, 1990). Although anatomically and functionally different, both the NAc core and shell are mainly comprised of GABAergic projection neurons known as medium spiny neurons (MSNs) (Matamales et al., 2009). Several studies have identified key morphologic differences between core and shell MSNs (Meredith et al., 1992; Forlano and Woolley, 2010) but few studies have directly addressed how core and shell MSNs differ in their intrinsic excitability (Pennartz et al., 1992; O'Donnell and Grace, 1993). Using whole-cell patch-clamp recordings in slices prepared from naive and rewarded male rats, we found that MSNs in the NAc shell were significantly more excitable than MSNs in the NAc core in both groups. In the shell, MSNs had significantly greater input resistance, lower cell capacitance, and a greater sag. This was accompanied by a lower action potential current threshold, a greater number of action potentials, and faster firing frequency compared with core MSNs. These subregional differences in intrinsic excitability could provide a potential physiological link to the distinct anatomic characteristics of core and shell MSNs and to their distinct functional roles in reward learning (Zahm, 1999; Ito and Hayen, 2011; Saddoris et al., 2015; West and Carelli, 2016).

**Key words:** electrophysiology; GABAergic; patch clamp; reward; ventral striatum

## Significance Statement

The nucleus accumbens (NAc) is a critical structure in the integration process of reward information necessary to regulate motivated behaviors. It has been divided into two main subregions known as the core and shell. The intrinsic excitability state of medium spiny neurons (MSNs), the main neuronal population of the NAc core and shell, can heavily influence how the NAc encodes and relays reward information. Understanding how the different subregions of the NAc respond to input stimuli by studying their intrinsic excitability is crucial for further dissecting the functional segregation of the NAc subregions in reward learning and ultimately linking it to disorders like addiction and anxiety.

Received October 22, 2022; accepted March 29, 2023; First published May 8, 2023.

The authors declare no competing financial interests.

Author contributions: C.E.M., G.G.M., and J.D.M. designed research; C.E.M. performed research; C.E.M. analyzed data; C.E.M., G.G.M., and J.D.M. wrote the paper.

## Introduction

The nucleus accumbens (NAc) is a part of the ventral striatum located within the basal forebrain. Decades of research have identified a fundamental role for the NAc in reward and motivation, making it a crucial structure for understanding numerous neuropsychiatric disorders including addiction, anxiety, depression, and bipolar disorder (Day and Carelli, 2007; Floresco, 2015; Salgado and Kaplitt, 2015). Based on differences in cellular arrangement, density, and connectivity, previous anatomic and histologic studies have divided the NAc into three subregions: core, shell, and rostral pole, where core and shell are indistinguishable (Záborszky et al., 1985; Berendse and Groenewegen, 1990; Zahm and Heimer, 1990). For example, some studies have shown that neurons in the NAc core and shell differ in their morphology with cells in the core having greater total surface area, dendritic branching, and spine density than cells in the shell (Meredith et al., 1992; Forlano and Woolley, 2010). Additionally, core and shell neurons show substantial differences in both afferent and efferent connections with striatal, mesencephalic, hypothalamic, amygdalar, cortical, and hippocampal regions (Záborszky et al., 1985; Berendse and Groenewegen, 1990; Zahm and Heimer, 1990; Heimer et al., 1991; Berendse et al., 1992; Meredith et al., 1992; Britt et al., 2012). Collectively, these subregional differences in NAc anatomy and connectivity, may be responsible for the distinctive functional roles in reward and motivation attributed to the core and shell (Zahm, 1999). These include functional differences in instrumental learning, Pavlovian conditioned approach, reward devaluation, impulsivity, as well as food-seeking and cocaine-seeking behaviors (Day and Carelli, 2007; Floresco, 2015).

Approximately 95% of the neurons in both the core and the shell of the NAc are GABAergic projection neurons known as medium spiny neurons (MSNs; Matamales et al., 2009). Within subregions, many electrophysiological studies have thoroughly characterized the intrinsic excitability properties of MSNs in rodents, including how these vary by sex (Cao et al., 2018; Proaño et al., 2018), estrous cycle (Proaño et al., 2018; Proaño and Meitzen, 2020), and neuronal subtype (Cao et al., 2018; Deroche et al., 2020), how they are modulated by dopamine (O'Donnell and Grace, 1996; Perez et al., 2006; Podda et al., 2010), and substances like cocaine (Kourrich and Thomas, 2009), and how they are altered in models of addiction (Mu et al., 2010; Graves et al., 2015), obesity (Alonso-Caraballo and Ferrario, 2019; Oginsky and Ferrario, 2019), stress, and depression

This work was supported by National Institute on Drug Addiction Grant R01 DA044960, the National Institute of Neurological Disorders and Stroke Grant F99 NS120544, the Taubman Emerging Scholar Fund Grant G022581, the Kenneth and Frances Eisenberg Award G021877, National Institute on Aging Grants R01 AG074552 and R01 AG052934, the National Institute of Mental Health Grant U19 MH106434, and the National Science Foundation Research Graduate Research Fellowship Program.

Correspondence should be addressed to Jonathan D. Morrow at [jonmorro@med.umich.edu](mailto:jonmorro@med.umich.edu) or Geoffrey G. Murphy at [murphyg@umich.edu](mailto:murphyg@umich.edu).

<https://doi.org/10.1523/ENEURO.0432-22.2023>

Copyright © 2023 Maria-Rios et al.

This is an open-access article distributed under the terms of the Creative Commons Attribution 4.0 International license, which permits unrestricted use, distribution and reproduction in any medium provided that the original work is properly attributed.

(Francis et al., 2015, 2019). Despite all the anatomic and functional evidence suggesting physiological differences between NAc subregions, very few studies have directly investigated how core and shell MSNs differ with one another in their passive and active intrinsic excitability properties. Previous findings in mice suggest that differences in input resistance between core and shell MSNs may result in greater excitability in shell MSNs (Kourrich and Thomas, 2009). In comparison, studies in rats have suggested very subtle and contrasting subregional differences, leaving uncertainty as to what the physiological differences between core and shell MSNs may be (Pennartz et al., 1992; O'Donnell and Grace, 1993).

For this study, we used whole-cell patch-clamp recordings to conduct a comprehensive electrophysiological analysis of the passive and active membrane properties of MSNs in the NAc core and shell of adult male rats. Since behavioral and environmental enrichment is known to alter intrinsic excitability of certain neuronal subtypes like MSNs in the NAc (Scala et al., 2018) and pyramidal neurons in the hippocampus (Malik and Chattarji, 2012; Valero-Aracama et al., 2015), we not only studied “naive” animals, but also rats that underwent six sessions of unpaired cue/food reward exposures (“rewarded”). The goal of our study is to characterize subregional physiological differences between the core and shell of the NAc in naive rats and explore whether these remain stable in “rewarded” rats that underwent behavioral enrichment.

## Materials and Methods

### Animals

All animal procedures were previously approved by the University Committee on the Use and Care of Animals (University of Michigan, Ann Arbor, MI). Thirty-one adult male Sprague Dawley rats (seven to eight weeks) were purchased from Charles River Laboratories (C72, R04) and housed in pairs. Rats were maintained on a 12/12 h light/dark cycle, and food and water were available *ad libitum* for the entirety of experimentation. Rats were divided into two counterbalanced groups before the study began: Naive ( $n = 13$ ) and Rewarded ( $n = 18$ ). Naive rats remained in their home cages and received no handling before electrophysiological recordings. Rewarded rats were acclimatized to the housing colony for at least 2 d before handling. After behavioral testing the rats remained in their home cages for a baseline period of one to three weeks before electrophysiological recordings.

### Drugs

Isoflurane (Fluriso - VetOne) was administered at 5% via inhalation for inducing anesthesia. PicROTOXIN (Tocris Bioscience) was dissolved in artificial CSF (ACSF) to make a 100  $\mu$ M solution. Kynurenic acid (Sigma-Aldrich) was dissolved in ACSF to make a 5 mM solution.

### Behavioral testing apparatus

Sixteen modular operant conditioning chambers (24.1 cm in width  $\times$  20.5 cm in depth  $\times$  29.2 cm in height; MED

Associates) were used for behavioral enrichment. Each chamber was in a sound-attenuating cubicle equipped with a ventilation fan to provide ambient background noise. Each chamber was equipped with a food magazine, a retractable lever (counterbalanced on the left or right side of the magazine), and a red house light on the wall opposite of the magazine. The magazine contained an infrared sensor to detect magazine entries, and the levers were calibrated to detect lever deflections in response to 10 g of applied weight. Whenever a lever was extended into the chamber, an LED mounted inside the lever mechanism illuminated the slot through which the lever protruded (ABET II Software; Lafayette Instrument).

### Behavioral testing procedure

Rats were not food deprived at any point during experimentation. All rats in the Rewarded group were habituated for 2 d before the start of training. Rats were handled individually and were familiarized with banana-flavored pellets (45 mg; Bio-Serv) in their home cages. On the third day, rats were placed into the test chambers for one pre-training session during which the red house-light remained on, but the lever was retracted. Twenty-five food pellets were delivered on a variable time (VT) 30-s schedule (i.e., one pellet was delivered on average every 30 s, but varied 0–60 s). Next, rats underwent six daily sessions of behavioral training. Each trial during a training session consisted of a presentation of the illuminated lever into the chamber for 10 s and a response-independent delivery of one pellet into the magazine. Both stimuli were on a VT 45-s schedule (i.e., time randomly varied 30–60 s between presentations). The beginning of the next intertrial interval commenced once both the lever and the pellet had been presented. Each test session consisted of 25 trials of random unpaired lever and pellet presentations. All rats consumed all the pellets that were delivered.

### Electrophysiology

#### *Slice preparation*

Rats were deeply anesthetized with isoflurane (Kent Scientific) and euthanized by decapitation. The brain was rapidly dissected and glued on a platform submerged in an ice-cold oxygenated (95% O<sub>2</sub>/5% CO<sub>2</sub>) cutting solution containing (in mM): 206 sucrose (Sigma-Aldrich), 10 D-glucose (Sigma-Aldrich), 1.25 NaH<sub>2</sub>PO<sub>4</sub> (Sigma-Aldrich), 26 NaHCO<sub>3</sub> (Sigma-Aldrich), 2 KCl (Fisher Chemical), 0.4 sodium ascorbic acid (Sigma-Aldrich), 2 MgSO<sub>4</sub> (Sigma-Aldrich), 1 CaCl<sub>2</sub> (Sigma-Aldrich), and 1 MgCl<sub>2</sub> (Sigma-Aldrich). A mid-sagittal cut was made to divide the two hemispheres, and coronal brain slices (300 μm) were cut using a vibrating blade microtome (Leica VT1200). The brain slices were transferred to a holding chamber with oxygenated artificial CSF (ACSF) containing (in mM): 119 NaCl (Sigma-Aldrich), 2.5 KCl (Fisher Chemical), 1 NaH<sub>2</sub>PO<sub>4</sub> (Sigma-Aldrich), 26.2 NaHCO<sub>3</sub> (Sigma-Aldrich), 11 D-glucose (Sigma-Aldrich), 1 sodium ascorbic acid (Sigma-Aldrich), 1.3 MgSO<sub>4</sub> (Sigma-Aldrich), and 2.5 CaCl<sub>2</sub> (Sigma-Aldrich; ~295 mOsm, pH 7.2–7.3) at 37°C for 20 min and then room temperature for at least 40 min of rest. The slices were kept

submerged in oxygenated ACSF in a holding chamber at room temperature for up to 7–8 h after slicing.

#### *Electrophysiological recordings*

After at least 1 h of rest, slices were transferred to the recording chamber where they were perfused with oxygenated ACSF (32°C) containing 100 μM of GABA<sub>A</sub> receptor antagonist, picrotoxin (Tocris Bioscience) and 5 mM of kynurenic acid (Sigma-Aldrich) to block glutamatergic transmission. Recordings from the NAc core and medial shell were done in the same slices which were obtained between +1.00 and +1.70 mm anterior from bregma (Paxinos and Franklin, 2019). Cells were visualized using infrared differential interference contrast (IR-DIC) optics (Microscope: Olympus BX51; Camera: Dage-MIT). Whole-cell current clamp recordings were performed using borosilicate glass pipettes (O.D. 1.5 mm, I.D. 0.86 mm; Sutter Instruments) with a 4–7 MΩ open tip resistance. Pipettes were filled with a potassium gluconate-based internal solution containing (in mM): 122 K-gluconate (Sigma-Aldrich), 20 HEPES (Sigma-Aldrich), 0.4 EGTA (Sigma-Aldrich), 2.8 NaCl (Sigma-Aldrich), and 2 Mg<sup>2+</sup>ATP/0.3 Na<sub>2</sub>GTP (~280 mOsm, pH adjusted to 7.2 with KOH). Medium spiny neurons were identified based on morphology (medium-sized soma) as well as a hyperpolarized resting potential between –70 and –90 mV and inward rectification. Neurons exhibiting a resting potential out of the desired range, characteristics of fast-spiking interneurons, and irregular firing pattern were excluded. All recordings were obtained using the MultiClamp 700B (Molecular Devices) amplifier and Digidata 1550A (Molecular Devices) digitizer. Data were filtered at 2 kHz, digitized at 10 kHz, and were collected and analyzed using pClamp 10.0 software (Molecular Devices). Recordings were not adjusted for the calculated liquid junction potential of 15.8 mV.

To perform whole-cell recordings, membrane seals with a resistance >1 GΩ were achieved before breaking into the cell. Membrane capacitance (C<sub>m</sub>) and series resistance (R<sub>s</sub>) were compensated under voltage-clamp, and C<sub>m</sub> was recorded 1 min after breaking in. R<sub>s</sub> was recorded in voltage-clamp with an average of 31 ± 12 (MΩ) on entry and 29 ± 12 (MΩ; mean ± SD) once the recordings were finished. Firing properties were recorded under current-clamp, and input resistance (R<sub>i</sub>) was monitored online during each sweep with a –100-pA, 25-ms current injection separated by 100 ms from the current injection step protocols. The average R<sub>i</sub> across all sweeps is reported. Only cells with an R<sub>i</sub> that remained stable (Δ < 20%) were included in the analysis (Naive: n = 51, Rewarded: n = 78). All neurons underwent two recording protocols from their RMP to assess firing properties. To study spike number, spike frequency, voltage/current relationships, and sag ratios, neurons were subjected to a step protocol consisting of 500-ms current injections starting from –500 to +500 pA in 25-pA increments. Each sweep was separated by 4 s. Resting membrane potential (RMP) was reported as the average voltage from all sweeps at 5 ms. The number of spikes was determined by counting the number of individual spikes at each current injection. Firing frequency was determined by averaging the frequency (in Hz) between each two spikes for a given current injection. If a

neuron reached depolarization block, data for that cell were reported until the current injection before the depolarization block (2.5% of cells in core and 9.8% in shell). The steady-state voltage responses were measured 200 ms from the onset of stimulation for each subthreshold current injection step. Sag ratios were determined by the ratio of the peak voltage at the most hyperpolarized current injection ( $-500$  pA) over the steady-state response. A ratio of 1.00 would represent no sag, and therefore, the greater the ratio, the larger the sag. For voltage/current relationship, the voltage reported is the  $\delta$  between the steady-state and the baseline voltage 1 ms before onset of stimulation.

To study single action potential (AP) firing properties, neurons received 5-ms current injections in 25-pA increments until a single AP was elicited. Each sweep was separated by 4 s. Current to threshold (pA) was determined as the minimal current injection necessary to induce a single AP. The AP threshold (mV) was defined from 0 mV as the voltage at the AP inflection point. The  $\Delta$  RMP/AP threshold (mV) was determined by taking the difference between the RMP and the AP threshold determined by the AP inflection point. The AP amplitude (mV) was defined from 0 mV as the voltage at the peak of the AP overshoot. The  $\Delta$  RMP/AP amplitude (mV) was determined by taking the difference between the RMP and the AP amplitude measured from 0 mV. The  $\Delta$  AP threshold/AP amplitude (mV) was determined by taking the difference between the AP threshold and the AP amplitude. Finally, AP halfwidth (ms) was defined as the duration of the AP at half the voltage of the peak amplitude.

### Experimental design and statistical analysis

A total of 129 cells from 31 rats were included in the analysis. The naive group had a total of 13 rats, from which 31 cells were recorded from in the core of 13 rats (one to two slices/one to four cells per rat) and 20 cells in the shell of nine of the rats (one slice/one to three cells per rat). The rewarded group had a total of 18 rats, from which 47 cells were recorded from in the core of 18 rats (one to two slices/one to five cells per rat) and 31 cells in the shell of 14 of the rats (one to three slices/one to four cells per rat). A total of 49 cells (Naive:  $n = 25$ , Rewarded:  $n = 24$ ) were excluded from the analyses of sag ratio and voltage/current relationship curves. For these cells the step protocol ranged from  $-200$  to  $+500$  pA as opposed to  $-500$  to  $+500$  pA. They were excluded to keep the hyperpolarized current injection analysis homogeneous.

All offline analysis of electrophysiological recordings was performed using Clampfit 10.7 (Molecular Devices). Statistical analyses were made using GraphPad Prism 8 (Dotmatrix) and SPSS Statistics (IBM) software. RMP,  $C_m$ ,  $R_i$ , sag ratio, current to threshold, AP threshold,  $\Delta$ RMP/AP threshold, AP amplitude,  $\Delta$ RMP/AP amplitude,  $\Delta$ AP threshold/AP amplitude, and AP halfwidth were analyzed using two-way ANOVA with subregion (core vs shell) and group (naive vs rewarded) as independent variables. Sidak's *post hoc* test was used for multiple comparisons. Data are presented as mean  $\pm$  SEM with each data point representing an individual cell, and significance level was set at  $p < 0.05$ . Number of spikes, spike firing frequency, and voltage/

current relationship curves ( $-500$  to  $0$  pA,  $0$  to  $+100$  pA) were analyzed using linear mixed-effects model via restricted maximum likelihood (REML). Fixed effects were set for subregion (core, shell), group (naive, rewarded), current injection (V/I:  $-500$  to  $0$  pA,  $0$  to  $+100$  pA; AP:  $+50$  to  $+400$  pA), subregion  $\times$  group, subregion  $\times$  current injection, group  $\times$  current injection, and subregion  $\times$  group  $\times$  current injection. Multiple comparisons were made using Sidak's *post hoc* test. Based on the group  $\times$  subregion statistical report, planned comparisons using mixed-effects model via REML were done to obtain individual subregion statistics for naive (core vs shell) and rewarded (core vs shell) rats and group statistics for core (naive vs rewarded) and shell (naive vs rewarded). Fixed effects to obtain subregion statistics within groups were set for subregion (core, shell), current injection (V/I:  $-500$  to  $0$  pA,  $0$  to  $+100$  pA; AP:  $+50$  to  $+400$  pA), and subregion  $\times$  current injection. Fixed effects to obtain group statistics within subregion were set for group (naive, rewarded), current injection (V/I:  $-500$  to  $0$  pA,  $0$  to  $+100$  pA; AP:  $+50$  to  $+400$  pA), and group  $\times$  current injection. Data are presented as mean  $\pm$  SEM with significance level set at  $p < 0.05$ .

## Results

### NAC MSNs exhibit distinct passive membrane properties in the core versus shell subregions of both naive and rewarded rats

To characterize the intrinsic excitability properties of MSNs in the NAc core and shell, whole-cell electrophysiological recordings were performed in rat brain slices (see Table 1 for summary of data). To confirm the reliability of our findings across subregions, we recorded not only from naive rats, but also from rats that underwent six sessions of unpaired cue/reward exposures (Fig. 1). Electrophysiological analysis revealed differences in passive membrane properties between the two subregions in both naive and rewarded rats (Fig. 2). Input resistance was significantly greater in NAc shell MSNs compared with core MSNs (two-way ANOVA: main effect of subregion,  $p < 0.001$ ; see Table 2 for full statistical report). Consistent with this, cell capacitance was significantly lower in NAc shell MSNs compared with core MSNs of both naive and rewarded rats (two-way ANOVA: main effect of subregion,  $p < 0.0001$ ; see Table 2 for full statistical report). No significant differences were found in resting potential between NAc core and shell MSNs (two-way ANOVA: no main effect of subregion,  $p > 0.05$ ; see Table 2 for full statistical report).

### MSNs in the NAc shell exhibit greater sag ratios and larger changes in membrane potential in response to current injections than core MSNs of both naive and rewarded rats

To investigate potential subregional differences in active intrinsic excitability properties between the NAc core and shell, we analyzed membrane potential responses of MSNs to current injections from  $-500$  to  $+100$  pA in 25-pA increments, generating a voltage/current relationship curve. Consistent with our findings for passive membrane

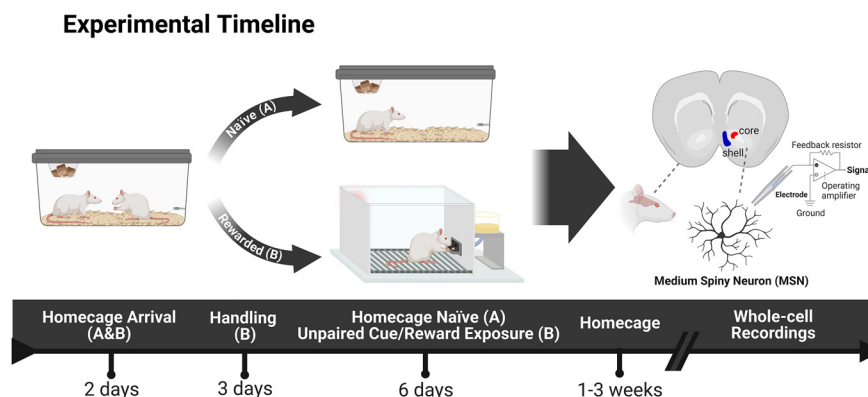


**Figure 1.** Experimental timeline. All rats were housed in pairs on arrival. The Naive group (A) was randomly selected and remained unhandled in their homecages for the entirety of the experiment until electrophysiological recordings were performed. The Rewarded group (B) was handled for 2 d after at least 2 d of acclimation to the housing room. They were then exposed to a pretraining session in the behavioral test apparatus where they received 25 pellets into a food-cup over the course of 30 min. For the following 6 d, they underwent a daily behavioral experience in which a neutral lever-cue was presented, and banana food pellet rewards were delivered into a food-cup randomly and independently of one another. Each session consisted of 25 independent trials of lever and reward presentations (ITI: 30–60 s). After the last session of unpaired cue/reward exposures, rats remained in their homecages for a period of one to three weeks. Subsequently, nucleus accumbens slices were prepared for whole-cell recordings of medium spiny neurons in the core and shell subregions. Behavioral responses for Rewarded rats were recorded and can be found in Extended Data Figure 1-1. Created with BioRender.

properties, NAc MSNs in the shell exhibited larger responses to current injections compared with responses recorded in core MSNs of both naive and rewarded rats (Fig. 3). The same hyperpolarizing ( $-500$ – $0$  pA) and depolarizing ( $0$ – $100$  pA) current injection steps consistently elicited a greater change in membrane potential in the shell than in the core, causing a significant shift of the V/I curve for both the naive and rewarded groups curve (hyperpolarizing: mixed-effects model: main effect of subregion,  $p < 0.0001$ ; depolarizing: mixed-effects model: main effect of subregion,  $p < 0.0001$ ; see Table 2 for full statistical report). In addition, we tested whether MSNs in the NAc core versus shell showed a significant difference in their voltage sag response to a  $-500$ -pA current injection (Fig. 3). To examine this further, a sag ratio was calculated by dividing the peak voltage response to  $-500$  pA over the steady-state response 200 ms from the onset of stimulation. In both naive and rewarded rats, MSNs in the NAc shell showed a greater sag ratio, representative of a larger sag, compared with MSNs in the NAc core (two-way ANOVA: main effect of subregion,  $p < 0.0001$ ; see Table 2 for full statistical report).

### NAc MSNs in the shell exhibit higher firing frequencies than core MSNs of both naive and rewarded rats as well as differences in action potential properties

To further examine the intrinsic excitability of core and shell MSNs of naive and rewarded rats, we measured firing rates in response to current injections from  $+50$  to  $+400$  pA in 25-pA increments. We found that in response to current injection steps of the same magnitude, MSNs in the shell had a significantly higher number of spikes (mixed-effects model: main effect of subregion,  $p < 0.0001$ ; see Table 2 for full statistical report) and greater firing frequency (mixed-effects model: main effect of subregion,  $p < 0.0001$ ) compared with MSNs in the NAc core in both the naive and

rewarded group (Fig. 4). In addition, MSNs in the core of naive rats showed a lower firing frequency compared with those in the rewarded group (mixed-effects model: main effect of group;  $p < 0.05$ ; see Table 2 for full statistical report) suggesting that the reward exposure experience may induce a slight increase in the excitability of MSNs in the NAc core.

To study single spike properties in MSNs in the NAc core and shell, neurons received 5-ms current injections in 25-pA increments until a single AP was elicited. Upon analysis, we found significant subregional differences in both naive and rewarded groups for most action potential properties (Fig. 5; Tables 1, 2). Consistent with the results above, the current necessary to elicit a single action potential was significantly lower in NAc shell MSNs compared with core MSNs (two-way ANOVA: main effect of subregion,  $p < 0.0001$ ; see Table 2 for full statistical report). Additionally, the AP threshold was significantly more depolarized in NAc shell MSNs compared with core MSNs of both naive and rewarded rats (two-way ANOVA: main effect of subregion,  $p < 0.001$ ; see Table 2 for full statistical report). Main effects of subregion were obtained for  $\Delta$  RMP/AP threshold, AP amplitude,  $\Delta$  RMP/AP amplitude, and  $\Delta$  AP threshold/AP amplitude, which all indicate a generally larger action potential threshold and smaller AP amplitude for shell MSNs compared with core MSNs. No significant differences were found for AP half-width (see Tables 1, 2 for statistical report).

## Discussion

Our data show that MSNs in the core and shell differ in their passive and active membrane properties. Overall, MSNs within the medial NAc shell are significantly more excitable than MSNs in the NAc core. In particular, we found that shell MSNs had greater input resistance and

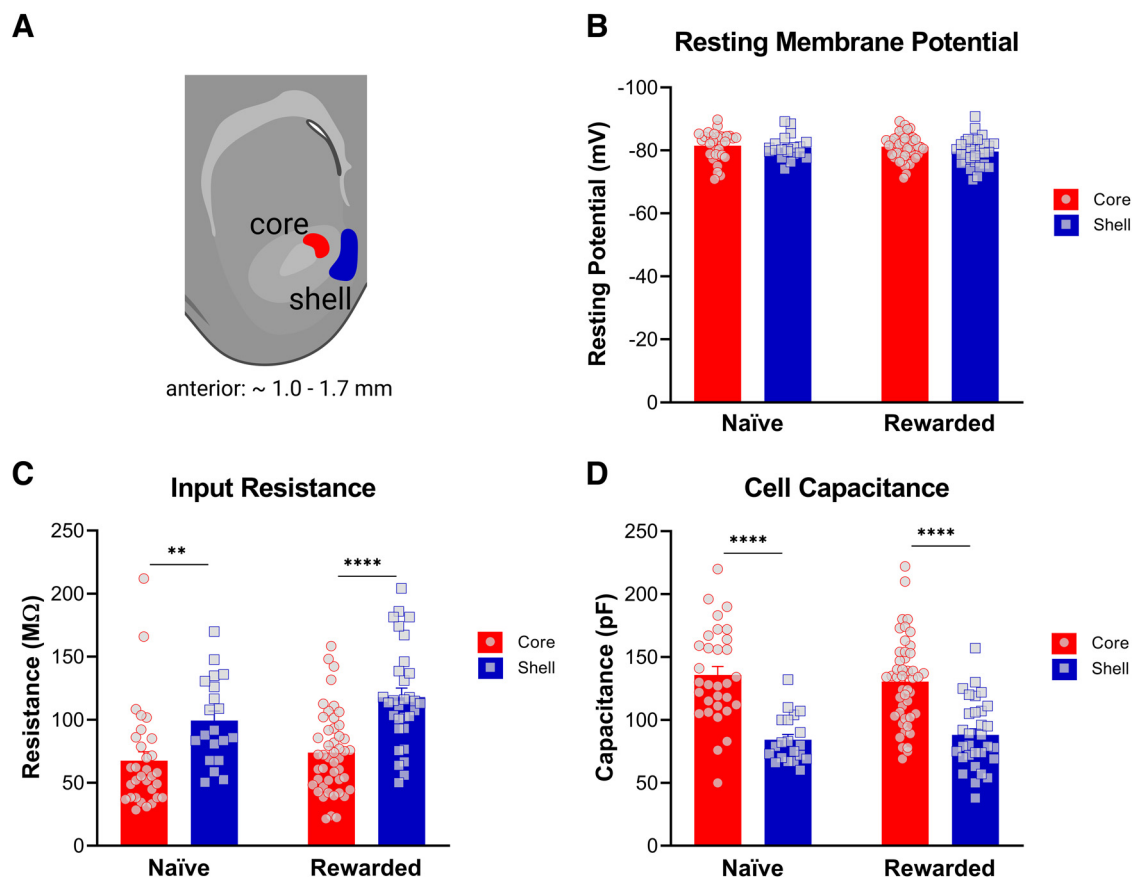


**Figure 2.** Nucleus accumbens (NAc) medium spiny neurons (MSNs) exhibit distinct passive membrane properties in the core versus shell subregions of both naive and rewarded rats. **A**, Representative diagram of coronal brain section containing the NAc core (red) and medial shell (blue) subregions (created with BioRender). Whole-cell patch-clamp recordings from medium spiny neurons were obtained from the highlighted areas. **B**, Resting potential. No significant differences were found in resting potential between NAc core and shell (two-way ANOVA: no main effect of subregion,  $p > 0.05$ ). **C**, Input resistance. In both naive and rewarded groups, input resistance was significantly greater in NAc shell MSNs compared with core MSNs (two-way ANOVA: main effect of subregion,  $p < 0.001$ ). **D**, Cell capacitance was significantly lower in NAc shell MSNs compared with core MSNs of both naive and rewarded rats (two-way ANOVA: main effect of subregion,  $p < 0.0001$ ). Significance for Sidak's *post hoc* test is shown as  $**p < 0.01$ ,  $****p < 0.0001$ . Each data point represents a single cell. Data are presented as mean  $\pm$  SEM. Please refer to Table 2 for complete statistical report.

lower cell capacitance compared with core MSNs. We also found a significant difference in the voltage/current relationship, with shell MSNs consistently showing a greater deflection in membrane potential in response to hyperpolarizing and depolarizing current injections. This was accompanied by a greater sag ratio for shell MSNs, which is a measure of the hyperpolarization-activated cation current, or Ih (Pape, 1996; Robinson and Siegelbaum, 2003). As expected, we found that shell MSNs exhibited a greater number of action potentials in response to current injection steps as well as greater firing frequency compared with core MSNs. The current necessary to induce a single action potential was also lower for shell MSNs. Interestingly, we found subregional differences between the action potential properties. Core MSNs had a significantly more hyperpolarized action potential threshold, and overall, a larger action potential amplitude as measured from zero, resting, and the threshold potential.

Since behavioral and environmental enrichment have been previously reported to induce changes and adaptations in

neuronal excitability of pyramidal neurons in the hippocampus (Malik and Chattarji, 2012; Valero-Aracama et al., 2015) as well as in MSNs in the NAc (Scala et al., 2018), we wanted to determine how stable subregional differences between core and shell would be regardless of the behavioral experience of the rats. We therefore recorded from core and shell MSNs of brain slices from both "naive" rats and "rewarded" rats that underwent six sessions of unpaired cue/reward exposures. Subregional differences in intrinsic excitability were highly consistent between the naive and rewarded groups. There were no significant differences in the number of action potentials, voltage/current relationship, or input resistance. However, naive animals had a lower firing frequency of core MSNs compared with rewarded animals. This suggests that reward exposures may have caused a slight increase in the excitability of core MSNs, consistent with previously reported *in vivo* changes in response to food rewards during learning tasks (Carelli, 2002; Day et al., 2006). It is worth noting that a resting period of one to three weeks following the unpaired CS-US task was imposed for the rewarded group

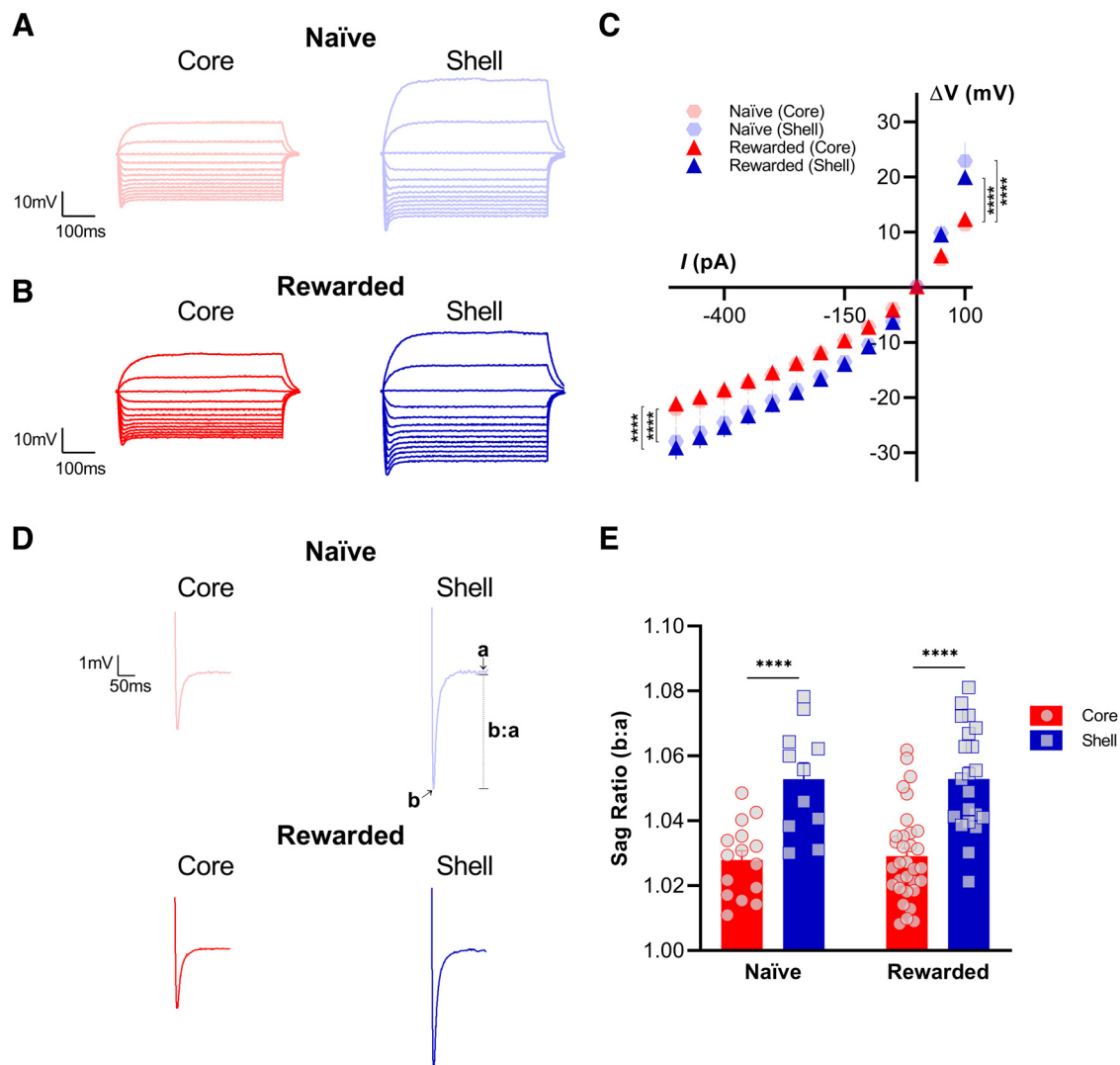


**Figure 3.** Nucleus accumbens (NAc) medium spiny neurons (MSNs) in the shell exhibit greater sag ratios and larger changes in membrane potential in response to current injections than core MSNs of both naive and rewarded rats. Representative voltage response traces from current-clamp recordings of MSNs in NAc core (left) and shell (right) slices from **(A)** naive and **(B)** rewarded rats. Current injection step protocol ranged from  $-500$  to  $+100$  pA and is shown here in  $50$ -pA increments. **C**, Voltage/current (V/I) relationship curve is significantly different between NAc shell and core MSNs of both naive and rewarded rats. The same hyperpolarizing ( $-500$ – $0$  pA) and depolarizing ( $0$ – $100$  pA) current injection steps consistently elicited a greater change in membrane potential in the shell versus in the core, causing a significant shift of the V/I curve (hyperpolarizing: mixed-effects model: main effect of subregion,  $p < 0.0001$ ; depolarizing: mixed-effects model: main effect of subregion,  $p < 0.0001$ ). **D**, Representative current-clamp recordings of voltage sag response to a  $-500$ -pA current injection from MSNs of NAc core (left) and shell (right) slices from naive (top) and rewarded (left) rats. Traces are shown as the average from all cells for each group and subregion. **E**, Sag ratio (b:a) was obtained by dividing the peak voltage response to a  $-500$ -pA current injection (b) over the steady-state response  $200$  ms from the onset of stimulation (a). In both naive and rewarded rats, MSNs in the NAc shell showed a greater sag ratio, representative of a larger sag, compared with MSNs in the NAc core (two-way ANOVA: main effect of subregion,  $p < 0.0001$ ). Significance for mixed-effect model planned comparison (**C**) and Sidak's *post hoc* test (**E**) is shown as \*\*\*\* $p < 0.0001$ . Each data point represents a single cell. Data are presented as mean  $\pm$  SEM. Please refer to Table 2 for complete statistical report.

rats. The purpose was to allow enough time to focus on intrinsic and not altered excitability differences between the rewarded and naive groups. We acknowledge that the impact on excitability of the reward exposures could have lingered regardless of the resting period, but the subtle difference reported between the two groups makes such lingering effects seem unlikely. Therefore, we focus on highlighting the finding that subregional excitability differences of core and

shell MSNs are stable and not very sensitive to simple behavioral experiences. Another important note is that though these subregional differences were very pronounced in both groups, it remains unknown whether they would be present in female rats, as we only studied male rats. Previous studies have reported excitability differences in the NAc of male and female rats that are particularly vulnerable to sex hormones (Cao et al., 2018; Proaño et al., 2018). Therefore, it is

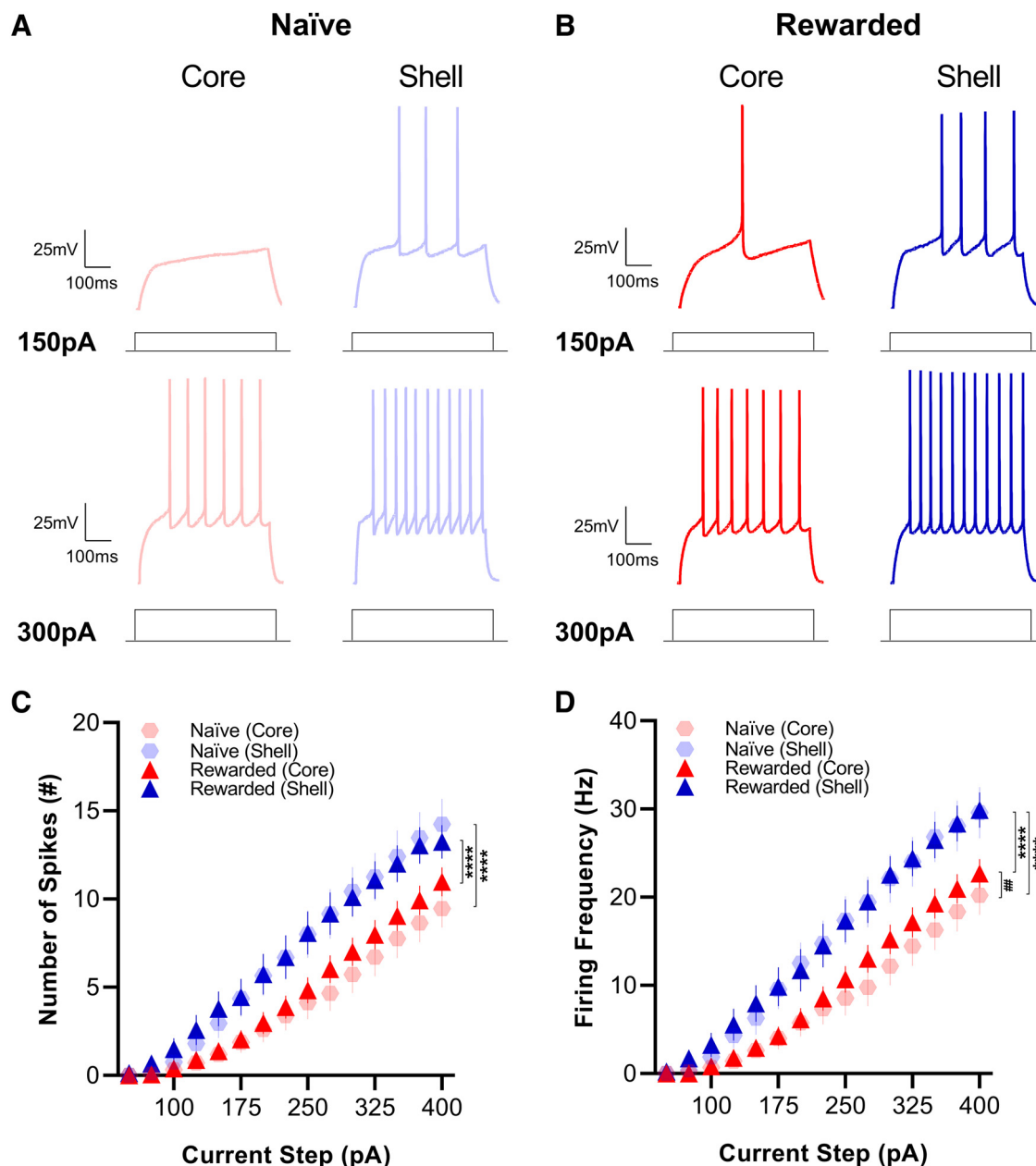


**Figure 4.** Medium spiny neurons (MSNs) located in the shell exhibit greater excitability than core MSNs of both naïve and rewarded rats. Representative traces of current-clamp recordings from MSNs in NAC core (left) and shell (right) slices of **(A)** naïve and **(B)** rewarded rats in response to 150-pA (top) and 300-pA (bottom) current injections. **C**, Number of spikes. MSNs in the NAC shell showed a higher number of spikes compared with MSNs in the NAC core in response to current injection steps of the same magnitude (mixed-effects model: main effect of subregion,  $p < 0.0001$ ). **D**, Firing frequency. Similarly, MSNs in the NAC shell showed greater firing frequency compared with MSNs in the NAC core in response to current injection steps of the same magnitude (mixed-effects model: main effect of subregion,  $p < 0.0001$ ). MSNs in the core of naïve rats also had lower firing frequency compared with those in the rewarded group (mixed-effects model: main effect of group;  $p < 0.05$ ). Significance for mixed-effect model planned comparison is shown as \*\*\*\* $p < 0.0001$ , ## $p < 0.01$ . Data are presented as mean  $\pm$  SEM. Please refer to [Table 2](#) for complete statistical report.

possible that this could translate to differential core versus shell subregional excitability in female rats.

The reported findings are consistent with known anatomic and morphologic differences between core and shell MSNs. Some studies have shown that neurons in the shell have significantly fewer dendritic arbors, branch segments, terminal segments, and lower spine densities

than those in the core (Meredith et al., 1992; O'Donnell and Grace, 1993; Forlano and Woolley, 2010; Wissman et al., 2011). These morphologic differences result in some shell MSNs having up to ~50% less surface area than core MSNs (Meredith et al., 1992). A lower surface area can result in significantly lower cell capacitance and consequently greater input resistance, providing a direct link



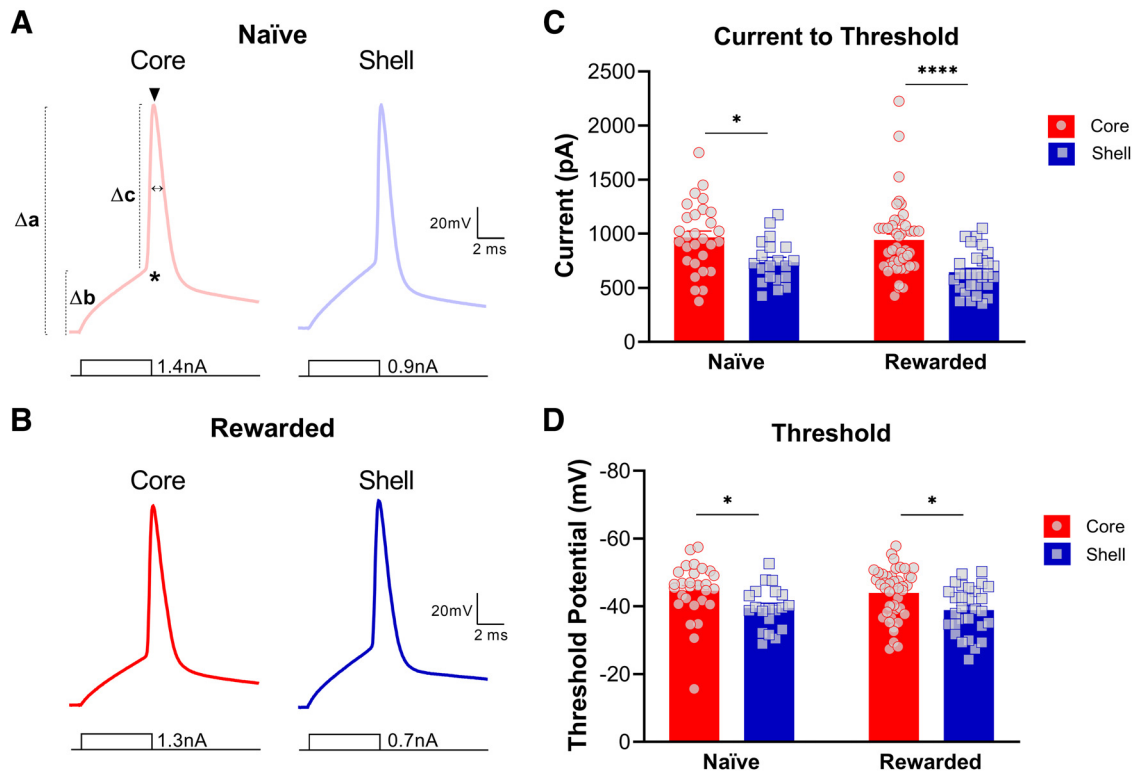


**Figure 5.** Nucleus accumbens (NAC) medium spiny neurons (MSNs) exhibit distinct action potential properties in the core versus shell subregions of both naive and rewarded rats. Representative single action potential traces of current-clamp recordings from MSNs in NAC core (left) and shell (right) slices of **(A)** naive and **(B)** rewarded rats. Symbols illustrated on A (left) represent the following: \* = AP threshold (mV),  $\Delta b$  =  $\Delta$  RMP/AP threshold (mV),  $\blacktriangledown$  = AP amplitude (mV),  $\Delta a$  =  $\Delta$  RMP/AP amplitude (mV),  $\Delta c$  =  $\Delta$  AP threshold/AP amplitude (mV),  $\leftrightarrow$  = AP halfwidth (ms). **C**, Current to threshold: In both naive and rewarded groups, the current necessary to elicit a single action potential was significantly lower in NAC shell MSNs compared with core MSNs (two-way ANOVA: main effect of subregion,  $p < 0.0001$ ). **D**, Action potential threshold. AP threshold was significantly more depolarized in NAC shell MSNs compared with core MSNs of both naive and rewarded rats (two-way ANOVA: main effect of subregion,  $p < 0.001$ ). Significance for Sidak's *post hoc* test is shown as \* $p < 0.05$ , \*\*\*\* $p < 0.0001$ . Each data point represented a single cell. Data are presented as mean  $\pm$  SEM. Please refer to Table 2 for complete statistical report.

**Table 1: Electrophysiological passive and active properties of medium spiny neurons in the core and shell of nucleus accumbens of naive and rewarded animals**

	Naive		Statistics <i>t/F, p</i>	Rewarded		Statistics <i>t/F, p</i>
	Core	Shell		Core	Shell	
<b>Passive membrane properties</b>						
Resting membrane potential, mV	-81.5 $\pm$ 0.8 (31)	-80.0 $\pm$ 0.8 (20)	0.48, 0.86	-81.2 $\pm$ 0.6 (47)	-79.7 $\pm$ 0.8 (31)	1.60, 0.21
Cell capacitance, pF	136 $\pm$ 7 (31)	84 $\pm$ 4 (20)	5.66, <0.0001	130 $\pm$ 5 (47)	88 $\pm$ 5 (31)	5.79, <0.0001
Input resistance, M $\Omega$	67 $\pm$ 7 (31)	99 $\pm$ 8 (20)	3.07, 0.0053	74 $\pm$ 5 (47)	118 $\pm$ 7 (31)	5.23, <0.0001
<b>Active membrane properties</b>						
V/I curve (-500 to 0 pA)	-12.0 $\pm$ 0.3 (15)	-17.2 $\pm$ 0.4 (11)	55.8, 3.61 <sup>-13</sup>	-12.7 $\pm$ 0.2 (33)	-17.7 $\pm$ 0.3 (21)	227, 8.66 <sup>-47</sup>
V/I curve (0 to +100 pA)	5.4 $\pm$ 0.5 (15)	10.8 $\pm$ 0.6 (11)	40.4, 4.11 <sup>-9</sup>	6.1 $\pm$ 0.3 (33)	9.8 $\pm$ 0.4 (21)	47.3, 4.65 <sup>-11</sup>
Sag ratio at -500 pA, mV	1.028 $\pm$ 0.003 (15)	1.053 $\pm$ 0.005 (11)	4.32, <0.0001	1.029 $\pm$ 0.002 (33)	1.053 $\pm$ 0.004 (21)	5.85, <0.0001
Number of spikes, AP#	3.2 $\pm$ 0.2 (31)	6.7 $\pm$ 0.3 (20)	72.8, 8.57 <sup>-17</sup>	4.5 $\pm$ 0.2 (47)	6.8 $\pm$ 0.2 (31)	66.6, 8.93 <sup>-16</sup>
Firing frequency, Hz	8.1 $\pm$ 0.4 (31)	14.5 $\pm$ 0.6 (20)	81.7, 1.48 <sup>-18</sup>	9.6 $\pm$ 0.4 (47)	14.9 $\pm$ 0.4 (31)	84.1, 2.25 <sup>-19</sup>
Current to threshold, pA	966 $\pm$ 58 (29)	737 $\pm$ 45 (20)	2.73, 0.014	943 $\pm$ 52 (43)	643 $\pm$ 36 (29)	4.32, <0.0001
AP threshold, mV (*)	-44 $\pm$ 1.5 (29)	-39.5 $\pm$ 1 (20)	2.37, 0.038	-44 $\pm$ 1 (43)	-39 $\pm$ 1 (29)	2.85, 0.010
$\Delta$ RMP/AP threshold, mV ( $\Delta b$ )	36 $\pm$ 1.6 (29)	41 $\pm$ 1.6 (20)	2.21, 0.056	37 $\pm$ 1 (43)	40 $\pm$ 1.6 (29)	1.64, 0.20
AP amplitude, mV ( $\blacktriangledown$ )	53 $\pm$ 1 (29)	50 $\pm$ 1 (20)	1.23, 0.39	53 $\pm$ 1 (43)	50 $\pm$ 1 (29)	2.01, 0.090
$\Delta$ RMP/AP amplitude, mV ( $\Delta a$ )	134 $\pm$ 1.6 (29)	131 $\pm$ 2 (20)	1.01, 0.53	134 $\pm$ 1 (43)	128 $\pm$ 1.5 (29)	2.64, 0.018
$\Delta$ AP threshold/AP amplitude, mV ( $\Delta c$ )	97 $\pm$ 2 (29)	90 $\pm$ 2 (20)	2.20, 0.059	97 $\pm$ 2 (43)	88 $\pm$ 2 (29)	2.94, 0.0078
AP halfwidth, ms ( $\leftrightarrow$ )	0.66 $\pm$ 0.01 (29)	0.68 $\pm$ 0.02 (20)	0.76, 0.70	0.68 $\pm$ 0.02 (43)	0.70 $\pm$ 0.02 (29)	0.62, 0.79

Table lists mean  $\pm$  SEM (sample size) for passive and active properties of core and shell MSNs for both naive and rewarded rats. Statistics for core versus shell comparisons were obtained from Sidak's *post hoc* test (*t* value, *p* value) and mixed-effects model planned comparisons (*F* value, *p* value). Main effects and interactions are detailed in Table 2.

**Table 2: Full statistical report for electrophysiological passive and active properties of medium spiny neurons in the core and shell of nucleus accumbens of naive and rewarded animals**

	Effects	<i>F</i> , <i>df</i> , <i>p</i>	<i>Post hoc</i> Comparison	<i>t/F</i> , <i>df</i> , <i>p</i>
<b>Figure 2</b>				
2B, resting membrane potential	Subregion (no main effect) <sup>a</sup>	$F_{(1,125)} = 1.90, p = 0.17$	-	-
2C, input resistance	Subregion (main effect) <sup>a</sup>	$F_{(1,125)} = 32.2, p < 0.0001$	Naive: core vs shell <sup>c</sup> Rewarded: core vs shell <sup>c</sup>	$t_{(125)} = 3.067, p = 0.0053$ $t_{(125)} = 5.232, p < 0.0001$
2D, cell capacitance	Subregion (main effect) <sup>a</sup>	$F_{(1,125)} = 64.6, p < 0.0001$	Naive: core vs shell <sup>c</sup> Rewarded: core vs shell <sup>c</sup>	$t_{(125)} = 5.661, p < 0.0001$ $t_{(125)} = 5.789, p < 0.0001$
<b>Figure 3</b>				
3C, voltage/current curve	Subregion (main effect) <sup>b</sup>	$F_{(1,1596)} = 224, p = 1.48 \times 10^{-47}$	Naive: core vs shell <sup>b</sup>	$F_{(1,504)} = 55.8, p = 3.61 \times 10^{-13}$
Hyperpolarizing: -500-0 pA	Current injection (main effect) <sup>b</sup>	$F_{(20,1596)} = 109, p = 1.02 \times 10^{-281}$	Rewarded: core vs shell <sup>d</sup>	$F_{(1,1092)} = 227, p = 8.66 \times 10^{-47}$
Depolarizing: 0-100 pA	Subregion × current injection (interaction) <sup>b</sup>	$F_{(20,1793)} = 1.68, p = 0.03$	Naive: core vs shell <sup>b</sup>	$F_{(1,117)} = 40.4, p = 4.11 \times 10^{-9}$
	Subregion (main effect) <sup>b</sup>	$F_{(1,375)} = 86.8, p = 1.06 \times 10^{-18}$	Rewarded: core vs shell <sup>d</sup>	$F_{(1,258)} = 47.3, p = 4.65 \times 10^{-11}$
	Current injection (main effect) <sup>b</sup>	$F_{(4,375)} = 142, p = 9.26 \times 10^{-74}$		
	Subregion × current injection (interaction) <sup>b</sup>	$F_{(4,375)} = 11.7, p = 6.17 \times 10^{-9}$		
3E, sag ratio	Subregion (main effect) <sup>a</sup>	$F_{(1,76)} = 47.6, p < 0.0001$	Naive: core vs shell <sup>c</sup> Rewarded: core vs shell <sup>c</sup>	$t_{(76)} = 4.32, p < 0.0001$ $t_{(76)} = 5.86, p < 0.0001$
<b>Figure 4</b>				
4C, number of spikes	Subregion (main effect) <sup>b</sup>	$F_{(1,1793)} = 137, p = 1.34 \times 10^{-30}$	Naive: core vs shell <sup>b</sup>	$F_{(1,706)} = 72.8, p = 8.57 \times 10^{-17}$
	Current injection (main effect) <sup>b</sup>	$F_{(14,1793)} = 89.4, p = 2.17 \times 10^{-194}$	Rewarded: core vs shell <sup>d</sup>	$F_{(1,1087)} = 66.6, p = 8.93 \times 10^{-16}$
	Subregion × current injection (interaction) <sup>b</sup>	$F_{(14,1793)} = 2.55, p = 0.001$		
4D, firing frequency	Subregion (main effect) <sup>b</sup>	$F_{(1,1793)} = 162, p = 9.17 \times 10^{-36}$	Naive: core vs shell <sup>b</sup>	$F_{(1,706)} = 81.7, p = 1.48 \times 10^{-18}$
	Current injection (main effect) <sup>b</sup>	$F_{(14,1793)} = 97.7, p = 8.23 \times 10^{-209}$	Rewarded: core vs shell <sup>d</sup>	$F_{(1,1087)} = 84.1, p = 2.25 \times 10^{-19}$
	Group (main effect) <sup>b</sup>	$F_{(1,1793)} = 4.09, p = 0.043$	Core: Naive vs rewarded <sup>d</sup>	$F_{(1,1097)} = 7.38, p = 0.007$
	Subregion × current injection (interaction) <sup>b</sup>	$F_{(14,1793)} = 2.94, p = 0.0002$		
<b>Figure 5</b>				
5C, current to threshold	Subregion (main effect) <sup>a</sup>	$F_{(1,117)} = 23.6, p < 0.0001$	Naive: core vs shell <sup>c</sup> Rewarded: core vs shell <sup>c</sup>	$t_{(117)} = 2.73, p = 0.014$ $t_{(117)} = 4.32, p < 0.0001$
5D, threshold potential	Subregion (main effect) <sup>a</sup>	$F_{(1,117)} = 13.3, p = 0.0004$	Naive: core vs shell <sup>c</sup> Rewarded: core vs shell <sup>c</sup>	$t_{(117)} = 2.37, p = 0.038$ $t_{(117)} = 2.86, p = 0.01$
<b>Table 1 (not in figure)</b>				
Δ RMP/AP threshold	Subregion (main effect) <sup>a</sup>	$F_{(1,117)} = 7.59, p = 0.0068$	Naive: core vs shell <sup>c</sup> Rewarded: core vs shell <sup>c</sup>	$t_{(117)} = 2.22, p = 0.056$ $t_{(117)} = 1.64, p = 0.20$
AP amplitude	Subregion (main effect) <sup>a</sup>	$F_{(1,117)} = 5.0, p = 0.028$	Naive: core vs shell <sup>c</sup> Rewarded: core vs shell <sup>c</sup>	$t_{(117)} = 1.23, p = 0.39$ $t_{(117)} = 2.01, p = 0.090$
Δ RMP/AP amplitude	Subregion (main effect) <sup>a</sup>	$F_{(1,117)} = 6.07, p = 0.015$	Naive: core vs shell <sup>c</sup> Rewarded: core vs shell <sup>c</sup>	$t_{(117)} = 1.00, p = 0.53$ $t_{(117)} = 2.64, p = 0.018$
Δ AP threshold/AP amplitude	Subregion (main effect) <sup>a</sup>	$F_{(1,117)} = 12.7, p = 0.0005$	Naive: core vs shell <sup>c</sup> Rewarded: core vs shell <sup>c</sup>	$t_{(117)} = 2.20, p = 0.059$ $t_{(117)} = 2.94, p = 0.0078$
AP halfwidth	Subregion (no main effect) <sup>a</sup>	$F_{(1,117)} = 0.96, p = 0.33$	-	-

Table is organized by figures and lists analyses performed, main effects and interactions, as well as *post hoc* and planned comparisons for group and subregion effects.

<sup>a</sup>Two-way ANOVA

<sup>b</sup>Mixed-effects model

<sup>c</sup>Sidak's

<sup>d</sup>Planned comparison

between morphologic and physiological properties. These marked differences in input resistance may be the primary cause of the greater excitability of shell MSNs compared with core MSNs. Although many electrophysiological studies in MSNs have measured the sag index (Belleau and Warren, 2000; Dehorter et al., 2009; Proaño and Meitzen, 2020), this is the first study reporting a subregional difference in sag between core and shell MSNs. Greater hyperpolarized responses to negative current injections could be activating more hyperpolarization-activated cation channels (HCN), which are known to be expressed in the NAC

(Uchimura et al., 1990; Monteggia et al., 2000; Notomi and Shigemoto, 2004; Santos-Vera et al., 2013), thus resulting in a greater sag response in shell MSNs (Robinson and Siegelbaum, 2003). Studies have identified striatal cholinergic neurons whose spontaneous tonic firing is regulated by Ih and is sensitive to dopaminergic modulation (Bennett et al., 2000; Deng et al., 2007). Interestingly, the mRNA and protein expression of HCN subunits in the NAC is thought to be very low (Monteggia et al., 2000; Santos-Vera et al., 2013), and the role of the Ih current in the MSN neuronal population remains largely unknown (Uchimura et al.,

1990; Inoue et al., 2012). Nonetheless, cocaine sensitization increases the expression of HCN<sub>2</sub> in the NAc without affecting the surface/intracellular ratio (Santos-Vera et al., 2013, 2019), and inhibition of HCN in the NAc significantly reduces methamphetamine self-administration (Cao et al., 2016). Therefore, Ih current in the NAc may modulate neuronal excitability and network dynamics, thereby modulating the reinforcing effect of drugs.

Our data are consistent with previous electrophysiological studies in mice, which also reported shell MSNs to exhibit greater input resistance and overall greater number of action potentials compared with core MSNs (Kourrich and Thomas, 2009). In rats, direct core versus shell intrinsic excitability comparisons have been somewhat contradictory. Consistent with our findings and those found in mice, one study reported that core MSNs had lower input resistance as well as a more negative resting membrane potential compared with shell MSNs (Pennartz et al., 1992). Conversely, another study found that overall core and shell MSNs had very similar passive membrane properties, and that shell MSNs were less excitable than core MSNs (O'Donnell and Grace, 1993). These apparent inconsistencies could be because of methodological differences in slice electrophysiology. Nonetheless, some anatomic studies have also reported contrasting findings in the differences between core and shell MSN morphology (Záborszky et al., 1985). Interestingly, it seems that a medial to lateral gradient in spine density and branching exists within the shell. Neurons in the lateral portion of the shell more closely resemble the morphology of neurons in the core (Meredith et al., 1992), meaning that if these physiological differences are linked to morphologic differences, the location within each subregion is crucial for detecting specific differences in core versus shell intrinsic excitability properties. For example, this could suggest that the intrinsic excitability properties of MSNs within the lateral portion of the NAc shell could more closely resemble those from core MSNs, which could be further explored in subsequent studies. This could at least partially explain incongruent findings regarding core versus shell neuronal morphology and physiology.

In the core and shell of the NAc, MSNs differ not only in their morphology, but also in their distinctive patterns of connectivity with mesencephalic regions (Groenewegen and Russchen, 1984; Deutch et al., 1988; Heimer et al., 1991; Berendse et al., 1992; Meredith et al., 1995; Zahm, 1999; Breton et al., 2019). These anatomic differences are accompanied by heterogeneity in dopamine D<sub>1</sub> and D<sub>2</sub> receptor expression as well as dopamine levels and utilization in the core and shell subregions. Overall, several studies have found that D<sub>1</sub> receptors outnumber D<sub>2</sub> receptors in the shell, while in the core D<sub>2</sub> receptors are more abundant (Bardo and Hammer, 1991; Lu et al., 1998; Hasbi et al., 2020). In addition, tyrosine hydroxylase immunoreactivity indicates that the shell is more densely innervated by dopaminergic terminals (Zahm, 1992), and dopamine levels are greater in the shell compared with the core (Deutch and Cameron, 1992). These differences in D<sub>1</sub> and D<sub>2</sub> receptor expression can functionally impact neuronal excitability (Deroche et al., 2020). For example, activation of D<sub>1</sub>-like receptors of MSNs can increase MSN

depolarization by inhibiting Kir-channel K<sup>+</sup> currents (Podda et al., 2010) and by enhancing L-type Ca<sup>2+</sup> currents (Hernández-López et al., 1997). Although activation of D<sub>2</sub> in MSNs of the NAc can also increase depolarization of the resting membrane potential by decreasing K<sup>+</sup> leak currents, it has been shown to significantly decrease action potential firing via A-type K<sup>+</sup> currents (Perez et al., 2006) and L-type Ca<sup>2+</sup> currents (Hernandez-Lopez et al., 2000). Therefore, morphologic differences between core and shell MSNs might not be the only cause for the subregional differences in membrane properties, but distinctive modulation from the dopaminergic system may also impact neuronal excitability. Substances like cocaine (Kourrich and Thomas, 2009), morphine (Madayag et al., 2019), and nicotine (Nisell et al., 1997) have also been found to have distinctive impacts on core and shell MSN intrinsic excitability and synaptic activity, providing further evidence of physiological and functional differences in neuronal properties.

The NAc is a critical structure of the motive circuit as it converges both cortical and subcortical information during associative learning to ultimately process and regulate motivated behaviors (Day and Carelli, 2007; Floresco, 2015; Salgado and Kaplitt, 2015). The intrinsic excitability state of MSNs – how sensitive neurons are to changes in potential in response to input stimuli, can heavily influence how the NAc encodes and relays reward information (O'Donnell and Grace, 1996; Nicola et al., 2000). The subregional differences in intrinsic excitability reported here provide a potential physiological link to the different morphologic and anatomic characteristics of core and shell MSNs. This can be used to further inform investigations of their distinct roles in reward learning (Zahm, 1999; Ito and Hayen, 2011; Saddoris et al., 2015; West and Carelli, 2016) and in generating problematic behavioral responses linked to disorders like addiction (Di Chiara, 2002; Ito et al., 2004), anxiety (Dutta et al., 2021), and impulsivity (Pattij et al., 2007; Feja et al., 2014).

## References

- Alonso-Caraballo Y, Ferrario CR (2019) Effects of the estrous cycle and ovarian hormones on cue-triggered motivation and intrinsic excitability of medium spiny neurons in the nucleus accumbens core of female rats. *Horm Behav* 116:104583.
- Bardo MT, Hammer RP (1991) Autoradiographic localization of dopamine D1 and D2 receptors in rat nucleus accumbens: resistance to differential rearing conditions. *Neuroscience* 45:281–290.
- Belleau ML, Warren RA (2000) Postnatal development of electrophysiological properties of nucleus accumbens neurons. *J Neurophysiol* 84:2204–2216.
- Bennett BD, Callaway JC, Wilson CJ (2000) Intrinsic membrane properties underlying spontaneous tonic firing in neostriatal cholinergic interneurons. *J Neurosci* 20:8493–8503.
- Berendse HW, Groenewegen HJ (1990) Organization of the thalamostriatal projections in the rat, with special emphasis on the ventral striatum. *J Comp Neurol* 299:187–228.
- Berendse HW, Groenewegen HJ, Lohman AH (1992) Compartmental distribution of ventral striatal neurons projecting to the mesencephalon in the rat. *J Neurosci* 12:2079–2103.
- Breton JM, Charbit AR, Snyder BJ, Fong PTK, Dias EV, Himmels P, Lock H, Margolis EB (2019) Relative contributions and mapping of

- ventral tegmental area dopamine and GABA neurons by projection target in the rat. *J Comp Neurol* 527:916–941.
- Britt JP, Benaliouad F, McDevitt RA, Stuber GD, Wise RA, Bonci A (2012) Synaptic and behavioral profile of multiple glutamatergic inputs to the nucleus accumbens. *Neuron* 76:790–803.
- Cao DN, Song R, Zhang SZ, Wu N, Li J (2016) Nucleus accumbens hyperpolarization-activated cyclic nucleotide-gated channels modulate methamphetamine self-administration in rats. *Psychopharmacology (Berl)* 233:3017–3029.
- Cao J, Dorris DM, Meitzen J (2018) Electrophysiological properties of medium spiny neurons in the nucleus accumbens core of prepubertal male and female *Drd1a*-tdTomato line 6 BAC transgenic mice. *J Neurophysiol* 120:1712–1727.
- Carelli RM (2002) Nucleus accumbens cell firing during goal-directed behaviors for cocaine vs. ‘natural’ reinforcement. *Physiol Behav* 76:379–387.
- Day JJ, Carelli RM (2007) The nucleus accumbens and Pavlovian reward learning. *Neuroscientist* 13:148–159.
- Day JJ, Wheeler RA, Roitman MF, Carelli RM (2006) Nucleus accumbens neurons encode Pavlovian approach behaviors: evidence from an autoshaping paradigm. *Eur J Neurosci* 23:1341–1351.
- Dehorter N, Guigoni C, Lopez C, Hirsch J, Eusebio A, Ben-Ari Y, Hammond C (2009) Dopamine-deprived striatal GABAergic interneurons burst and generate repetitive gigantic IPSCs in medium spiny neurons. *J Neurosci* 29:7776–7787.
- Deng P, Zhang Y, Xu ZC (2007) Involvement of *Ih* in dopamine modulation of tonic firing in striatal cholinergic interneurons. *J Neurosci* 27:3148–3156.
- Deroche MA, Lassalle O, Castell L, Valjent E, Manzoni OJ (2020) Cell-type- and endocannabinoid-specific synapse connectivity in the adult nucleus accumbens core. *J Neurosci* 40:1028–1041.
- Deutch AY, Cameron DS (1992) Pharmacological characterization of dopamine systems in the nucleus accumbens core and shell. *Neuroscience* 46:49–56.
- Deutch AY, Goldstein M, Baldino F, Roth RH (1988) Telencephalic projections of the A8 dopamine cell group. *Ann N Y Acad Sci* 537:27–50.
- Di Chiara G (2002) Nucleus accumbens shell and core dopamine: differential role in behavior and addiction. *Behav Brain Res* 137:75–114.
- Dutta S, Beaver J, Halcomb CJ, Jasnow AM (2021) Dissociable roles of the nucleus accumbens core and shell subregions in the expression and extinction of conditioned fear. *Neurobiol Stress* 15:100365.
- Feja M, Hayn L, Koch M (2014) Nucleus accumbens core and shell inactivation differentially affects impulsive behaviours in rats. *Prog Neuropsychopharmacol Biol Psychiatry* 54:31–42.
- Floresco SB (2015) The nucleus accumbens: an interface between cognition, emotion, and action. *Annu Rev Psychol* 66:25–52.
- Forlano PM, Woolley CS (2010) Quantitative analysis of pre- and postsynaptic sex differences in the nucleus accumbens. *J Comp Neurol* 518:1330–1348.
- Francis TC, Chandra R, Friend DM, Finkel E, Dayrit G, Miranda J, Brooks JM, Iñiguez SD, O’Donnell P, Kravitz A, Lobo MK (2015) Nucleus accumbens medium spiny neuron subtypes mediate depression-related outcomes to social defeat stress. *Biol Psychiatry* 77:212–222.
- Francis TC, Gaynor A, Chandra R, Fox ME, Lobo MK (2019) The selective RhoA inhibitor Rhosin promotes stress resiliency through enhancing D1-medium spiny neuron plasticity and reducing hyperexcitability. *Biol Psychiatry* 85:1001–1010.
- Graves SM, Clark MJ, Traynor JR, Hu X-T, Napier TC (2015) Nucleus accumbens shell excitability is decreased by methamphetamine self-administration and increased by 5-HT<sub>2C</sub> receptor inverse agonism and agonism. *Neuropharmacology* 89:113–121.
- Groenewegen H, Russchen FT (1984) Organization of the efferent projections of the nucleus accumbens to pallidal, hypothalamic, and mesencephalic structures: a tracing and immunohistochemical study in the cat. *J Comp Neurol* 223:347–367.
- Hasbi A, Sivasubramanian M, Milenkovic M, Komarek K, Madras BK, George SR (2020) Dopamine D1-D2 receptor heteromer expression in key brain regions of rat and higher species: upregulation in rat striatum after cocaine administration. *Neurobiol Dis* 143:105017.
- Heimer L, Zahm DS, Churchill L, Kalivas PW, Wohltmann C (1991) Specificity in the projection patterns of accumbal core and shell in the rat. *Neuroscience* 41:89–125.
- Hernández-López S, Vargas J, Surmeier DJ, Reyes A, Galarraga E (1997) D<sub>1</sub> receptor activation enhances evoked discharge in neostriatal medium spiny neurons by modulating an L-type Ca<sup>2+</sup> conductance. *J Neurosci* 17:3334–3342.
- Hernandez-Lopez S, Tkatch T, Perez-Garci E, Galarraga E, Vargas J, Hamm H, Surmeier DJ (2000) D2 dopamine receptors in striatal medium spiny neurons reduce L-type Ca<sup>2+</sup> currents and excitability via a novel PLC[ $\beta$ ]<sub>1</sub>-IP<sub>3</sub>-calcineurin-signaling cascade. *J Neurosci* 20:8987–8995.
- Inoue R, Aosaki T, Miura M (2012) Protein kinase C activity alters the effect of  $\mu$ -opioid receptors on inhibitory postsynaptic current in the striosomes. *NeuroReport* 23:184–188.
- Ito R, Hayden A (2011) Opposing roles of nucleus accumbens core and shell dopamine in the modulation of limbic information processing. *J Neurosci* 31:6001–6007.
- Ito R, Robbins TW, Everitt BJ (2004) Differential control over cocaine-seeking behavior by nucleus accumbens core and shell. *Nat Neurosci* 7:389–397.
- Kourrich S, Thomas MJ (2009) Similar neurons, opposite adaptations: psychostimulant experience differentially alters firing properties in accumbens core versus shell. *J Neurosci* 29:12275–12283.
- Lu XY, Behnam Ghasemzadeh M, Kalivas PW (1998) Expression of D1 receptor, D2 receptor, substance P and enkephalin messenger RNAs in the neurons projecting from the nucleus accumbens. *Neuroscience* 82:767–780.
- Madayag AC, Gomez D, Anderson EM, Ingebretson AE, Thomas MJ, Hearing MC (2019) Cell-type and region-specific nucleus accumbens AMPAR plasticity associated with morphine reward, reinstatement, and spontaneous withdrawal. *Brain Struct Funct* 224:2311–2324.
- Malik R, Chattarji S (2012) Enhanced intrinsic excitability and EPSP-spike coupling accompany enriched environment-induced facilitation of LTP in hippocampal CA1 pyramidal neurons. *J Neurophysiol* 107:1366–1378.
- Matamales M, Bertran-Gonzalez J, Salomon L, Degos B, Deniau J-M, Valjent E, Hervé D, Girault J-A (2009) Striatal medium-sized spiny neurons: identification by nuclear staining and study of neuronal subpopulations in BAC transgenic mice. *PLoS One* 4:e4770.
- Meredith GE, Agolia R, Arts MP, Groenewegen HJ, Zahm DS (1992) Morphological differences between projection neurons of the core and shell in the nucleus accumbens of the rat. *Neuroscience* 50:149–162.
- Meredith GE, Ypma P, Zahm DS (1995) Effects of dopamine depletion on the morphology of medium spiny neurons in the shell and core of the rat nucleus accumbens. *J Neurosci* 15:3808–3820.
- Monteggia LM, Eisch AJ, Tang MD, Kaczmarek LK, Nestler EJ (2000) Cloning and localization of the hyperpolarization-activated cyclic nucleotide-gated channel family in rat brain. *Brain Res Mol Brain Res* 81:129–139.
- Mu P, Moyer JT, Ishikawa M, Zhang Y, Panksepp J, Sorg BA, Schlüter OM, Dong Y (2010) Exposure to cocaine dynamically regulates the intrinsic membrane excitability of nucleus accumbens neurons. *J Neurosci* 30:3689–3699.
- Nicola SM, Surmeier DJ, Malenka RC (2000) Dopaminergic modulation of neuronal excitability in the striatum and nucleus accumbens. *Annu Rev Neurosci* 23:185–215.
- Nisell M, Marcus M, Nomikos GG, Svensson TH (1997) Differential effects of acute and chronic nicotine on dopamine output in the core and shell of the rat nucleus accumbens. *J Neural Transm (Vienna)* 104:1–10.
- Notomi T, Shigemoto R (2004) Immunohistochemical localization of *Ih* channel subunits, HCN1–4, in the rat brain. *J Comp Neurol* 471:241–276.

- O'Donnell P, Grace AA (1993) Physiological and morphological properties of accumbens core and shell neurons recorded in vitro. *Synapse* 13:135–160.
- O'Donnell P, Grace AA (1996) Dopaminergic reduction of excitability in nucleus accumbens neurons recorded in vitro. *Neuropsychopharmacology* 15:87–97.
- Oginsky MF, Ferrario CR (2019) Eating “junk food” has opposite effects on intrinsic excitability of nucleus accumbens core neurons in obesity-susceptible versus -resistant rats. *J Neurophysiol* 122:1264–1273.
- Pape HC (1996) Queer current and pacemaker: the hyperpolarization-activated cation current in neurons. *Annu Rev Physiol* 58:299–327.
- Pattij T, Janssen MCW, Vanderschuren LJMJ, Schoffelmeier ANM, van Gaalen MM (2007) Involvement of dopamine D1 and D2 receptors in the nucleus accumbens core and shell in inhibitory response control. *Psychopharmacology (Berl)* 191:587–598.
- Paxinos G, Franklin KBJ (2019) Paxinos and Franklin's the Mouse Brain in Stereotaxic Coordinates. Academic Press.
- Pennartz CMA, Dolleman-Van der Weel MJ, da Silva FHL (1992) Differential membrane properties and dopamine effects in the shell and core of the rat nucleus accumbens studied in vitro. *Neurosci Lett* 136:109–112.
- Perez MF, White FJ, Hu XT (2006) Dopamine D(2) receptor modulation of K<sup>+</sup> channel activity regulates excitability of nucleus accumbens neurons at different membrane potentials. *J Neurophysiol* 96:2217–2228.
- Podda MV, Riccardi E, D'Ascenzo M, Azzena GB, Grassi C (2010) Dopamine D1-like receptor activation depolarizes medium spiny neurons of the mouse nucleus accumbens by inhibiting inwardly rectifying K<sup>+</sup> currents through a cAMP-dependent protein kinase A-independent mechanism. *Neuroscience* 167:678–690.
- Proaño SB, Meitzen J (2020) Estradiol decreases medium spiny neuron excitability in female rat nucleus accumbens core. *J Neurophysiol* 123:2465–2475.
- Proaño SB, Morris HJ, Kunz LM, Dorris DM, Meitzen J (2018) Estrous cycle-induced sex differences in medium spiny neuron excitatory synaptic transmission and intrinsic excitability in adult rat nucleus accumbens core. *J Neurophysiol* 120:1356–1373.
- Robinson RB, Siegelbaum SA (2003) Hyperpolarization-activated cation currents: from molecules to physiological function. *Annu Rev Physiol* 65:453–480.
- Saddoris MP, Cacciapaglia F, Wightman RM, Carelli RM (2015) Differential dopamine release dynamics in the nucleus accumbens core and shell reveal complementary signals for error prediction and incentive motivation. *J Neurosci* 35:11572–11582.
- Salgado S, Kaplitt MG (2015) The nucleus accumbens: a comprehensive review. *Stereotact Funct Neurosurg* 93:75–93.
- Santos-Vera B, Vázquez-Torres R, García Marrero HG, Ramos Acevedo JM, Arencibia-Albite F, Vélez-Hernández ME, Miranda JD, Jiménez-Rivera CA (2013) Cocaine sensitization increases I<sub>h</sub> current channel subunit 2 (HCN<sub>2</sub>) protein expression in structures of the mesocorticolimbic system. *J Mol Neurosci* 50:234–245.
- Santos-Vera B, Vaquer-Alicea A del C, Maria-Rios CE, Montiel-Ramos A, Ramos-Cardona A, Vázquez-Torres R, Sanabria P, Jiménez-Rivera CA (2019) Protein and surface expression of HCN2 and HCN4 subunits in mesocorticolimbic areas after cocaine sensitization. *Neurochem Int* 125:91–98.
- Scala F, et al. (2018) Environmental enrichment and social isolation mediate neuroplasticity of medium spiny neurons through the GSK3 pathway. *Cell Rep* 23:555–567.
- Uchimura N, Cherubini E, North RA (1990) Cation current activated by hyperpolarization in a subset of rat nucleus accumbens neurons. *J Neurophysiol* 64:1847–1850.
- Valero-Aracama MJ, Sauvage MM, Yoshida M (2015) Environmental enrichment modulates intrinsic cellular excitability of hippocampal CA1 pyramidal cells in a housing duration and anatomical location-dependent manner. *Behav Brain Res* 292:209–218.
- West EA, Carelli RM (2016) Nucleus accumbens core and shell differentially encode reward-associated cues after reinforcer devaluation. *J Neurosci* 36:1128–1139.
- Wissman AM, McCollum AF, Huang G-Z, Nikrodhanond AA, Woolley CS (2011) Sex differences and effects of cocaine on excitatory synapses in the nucleus accumbens. *Neuropharmacology* 61:217–227.
- Záborszky L, Alheid GF, Beinfeld MC, Eiden LE, Heimer L, Palkovits M (1985) Cholecystokinin innervation of the ventral striatum: a morphological and radioimmunological study. *Neuroscience* 14:427–453.
- Zahm DS (1992) An electron microscopic morphometric comparison of tyrosine hydroxylase immunoreactive innervation in the neostriatum and the nucleus accumbens core and shell. *Brain Res* 575:341–346.
- Zahm DS (1999) Functional-anatomical implications of the nucleus accumbens core and shell subterritories. *Ann N Y Acad Sci* 877:113–128.
- Zahm DS, Heimer L (1990) Two transpallidal pathways originating in the rat nucleus accumbens. *J Comp Neurol* 302:437–446.